ResearchGate

See discussions, stats, and author profiles for this publication at: https://www.researchgate.net/publication/23288105

Time-Dependent Interactions of the Two Porphyrinic Compounds Chlorin e6 and Mono-L-aspartyl-chlorin e6 with Phospholipid Vesicles Probed by NMR Spectroscopy

ARTICLE *in* LANGMUIR · OCTOBER 2008

Impact Factor: 4.46 · DOI: 10.1021/la802040v · Source: PubMed

CITATIONS
15

READS
21

4 AUTHORS, INCLUDING:

Martina Vermathen
Universität Bern
22 PUBLICATIONS **515** CITATIONS
SEE PROFILE

Peter Vermathen
Inselspital, Universitätsspital Bern
99 PUBLICATIONS **1,859** CITATIONS
SEE PROFILE

Peter Bigler
Universität Bern
65 PUBLICATIONS **890** CITATIONS
SEE PROFILE

Available from: Martina Vermathen
Retrieved on: 30 January 2016

Time-Dependent Interactions of the Two Porphyrinic Compounds Chlorin e6 and Mono-L-aspartyl-chlorin e6 with Phospholipid Vesicles Probed by NMR Spectroscopy

Martina Vermathen,*,† Peter Vermathen,‡ Uschi Simonis,§ and Peter Bigler†

Department of Chemistry and Biochemistry, University of Bern, Freiestrasse 3, CH-3012 Bern, Switzerland, Department of Clinical Research (AMSM), MR-Center 1, University and Inselspital, CH-3010 Bern, Switzerland, and Department of Chemistry and Biochemistry, San Francisco State University, 1600 Holloway Avenue, San Francisco, California 94132

Received December 17, 2007. Revised Manuscript Received August 14, 2008

The distribution processes of chlorin e6 (CE) and monoaspartyl-chlorin e6 (MACE) between the outer and inner phospholipid monolayers of 1,2-dioleoyl-phosphatidylcholine (DOPC) vesicles were monitored by ^{1}H NMR spectroscopy through analysis of chemical shifts and line widths of the DOPC vesicle resonances. Chlorin adsorption to the outer vesicle monolayer induced changes in the DOPC ^{1}H NMR spectrum. Most pronounced was a split of the N-methyl choline resonance, allowing for separate analysis of inner and outer vesicle layers. Transbilayer distribution of the chlorin compounds was indicated by time-dependent characteristic spectral changes of the DOPC resonances. Kinetic parameters for the flip-flop processes, that is, half-lives and rate constants, were obtained from the experimental data points. In comparison to CE, MACE transbilayer movement was significantly reduced, with MACE remaining more or less attached to the outer membrane layer. The distribution coefficients for CE and MACE between the vesicular and aqueous phase were determined. Both CE and MACE exhibited a high affinity for the vesicular phase. For CE, a positive correlation was found between transfer rate and increasing molar ratio CE/DOPC. Enhanced membrane rigidity induced by increasing amounts of cholesterol into the model membrane was accompanied by a decrease of CE flip-flop rates across the membrane. The present study shows that the movement of porphyrins across membranes can efficiently be investigated by ^{1}H NMR spectroscopy and that small changes in porphyrin structure can have large effects on membrane kinetics.

Introduction

The interest in porphyrins interacting with membranes originates from their great potential as sensitizers in photodynamic therapy (PDT).[1] Over the past years, PDT has become a well-accepted treatment modality for various cancers as well as noncancerous diseases.[1−3] One of the advantages of PDT is its high dual selectivity.[4] On one hand, porphyrinic compounds selectively accumulate in proliferating tissue; on the other hand, tissue damage is only achieved if the three components, photosensitizer, light, and oxygen, are combined. The reasons for the selective uptake of porphyrinic compounds are not yet clear.[5] Mainly two potential mechanisms are reported in the literature: First, an overexpression of LDL receptors on the tumor cell surface may lead to enhanced uptake of LDL-bound porphyrins by receptor-mediated endocytosis.[1] Second, depending on their structure, passive diffusion of porphyrins with ionizable groups into tumor cells may be enhanced due to the slightly acidic extracellular pH of tumor tissue building up a pH gradient across the membrane.[6] However, besides these potential uptake pathways, it is generally accepted that subcellular membranes belong to the main targets of porphyrin-based sensitizers.[4] Thus, membrane penetration of porphyrinic drugs is believed to be one of the crucial factors for their efficiency in PDT.[7,8] Since both cellular uptake mechanisms and the determinants of subcellular localization patterns of porphyrinic compounds are still uncertain, systematic studies on porphyrin membrane interactions at the molecular level are of great interest. Elucidating the factors modulating porphyrin location and time-dependent distribution in the membrane will therefore enhance the knowledge about the principles underlying porphyrin membrane interactions and will ultimately aid to improve the development of effective photosensitizers.

Information about the time-dependence of the distribution of a porphyrinic compound across the membrane not only demonstrates its preferential localization sites but also allows one to draw conclusions with respect to its cell uptake mechanisms and subcellular distribution.[4] Thus, it has been postulated that slow distributing compounds are most likely taken up via the endocytotic pathway while faster distributing compounds may enter the cell by the passive diffusion mechanism.[9,10] To date, only a few porphyrins have been characterized with respect to their transbilayer movement. The data have usually been obtained from fluorescence spectroscopy, while to the best of our knowledge no nuclear magnetic resonance (NMR) spectroscopy studies have been performed so far to probe the kinetics of

* To whom correspondence should be addressed. Telephone: +41 031/631 4384. Fax: +41 031/631 3424. E-mail: martina.vermathen@ioc.unibe.ch.
† University of Bern.
‡ University and Inselspital.
§ San Francisco State University.

(1) MacDonald, I. J.; Dougherty, T. J. *J. Porphyrins Phthalocyanines* **2001**, *5*, 105–129.
(2) Dougherty, T. J.; Gomer, C. J.; Henderson, B. W.; Jori, G.; Kessel, D.; Korbelik, M.; Moan, J.; Peng, Q. *J. Natl. Cancer Inst.* **1998**, *90*, 898–905.
(3) Dougherty, T. J. *J. Clin. Laser Med. Surg.* **2002**, *20*, 3–7.
(4) Castano, A. P.; Demidova, T. N.; Hamblin, M. R. *Photodiagn. Photodyn. Ther.* **2004**, *1*, 279–293.
(5) Kessel, D. *Photodiagn. Photodyn. Ther.* **2004**, *1*, 3–7.
(6) Gerweck, L. E.; Vijayappa, S.; Kozin, S. *Mol. Cancer Ther.* **2006**, *5*, 1275–1279.
(7) Ricchelli, F. *J. Photochem. Photobiol., B* **1995**, *29*, 109–118.
(8) Lavi, A.; Weitman, H.; Holmes, R. T.; Smith, K. M.; Ehrenberg, B. *Biophys. J.* **2002**, *82*, 2101–2110.
(9) Maman, N.; Dhami, S.; Phillips, D.; Brault, D. *Biochim. Biophys. Acta* **1999**, *1420*, 168–178.
(10) Bonneau, S.; Morliere, P.; Brault, D. *Biochem. Pharmacol.* **2004**, *68*, 1443–1452.

10.1021/la802040v CCC: $40.75 © 2008 American Chemical Society
Published on Web 09/30/2008

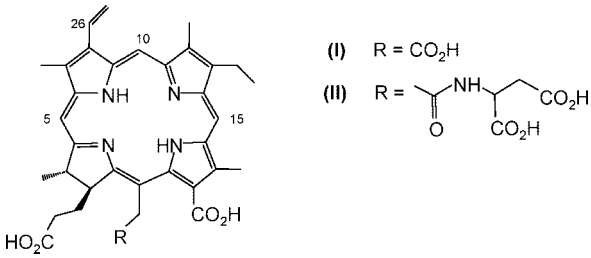

Figure 1. Structures of (I) chlorin e6 (CE) and (II) monoaspartyl-chlorin e6 (MACE).

porphyrin transbilayer movement. For example, detailed fluorescence data on membrane transfer are available for deuteroporphyrin, a dicarboxylic porphyrin which was found to rapidly distribute across the membrane,[11−14] while a disulfonated phthalocyanine was found to be retained in the outer monolayer.[9]

Here, we report on NMR spectroscopy measurements to determine chlorin distribution between the outer and inner phospholipid monolayers of a model membrane and to determine the factors modulating the kinetics. Among the porphyrinic compounds, chlorins have evolved as promising photosensitizers for PDT mainly due to their strong light absorption in the red wavelength region.[1,15] Moreover, the amphiphilic character of the porphyrin is a strong requirement for localization in the lipid phase of model membranes.[16,17] Both, chlorin e6 (CE) and monoaspartyl-chlorin e6 (MACE) are amphiphilic compounds bearing three and four peripheral carboxy groups, respectively, on one side of the chlorin macrocycle (Figure 1). Thus, besides their advantageous light absorbing properties, their amphiphilicity may enhance their membrane solubility.

In this paper, unilamellar phospholipid bilayer vesicles of intermediate size (50−60 nm in diameter) formed from 1,2-dioleoyl-phosphatidylcholine (DOPC, Figure 2) were used as model membranes. Owing to their dynamic properties, these vesicles provide membrane mimicking systems well suited for NMR spectroscopic investigations in the solution state, giving rise to sufficiently well-resolved isotropic lines.[18,19] NMR studies have been successfully applied to study the transport of various compounds across such lipid bilayer membranes or to investigate factors modulating membrane permeability.[20−25] Usually, NMR signals of the incorporated compound have been evaluated for this purpose, partially with the aid of paramagnetic shift reagents,[23−25] or the membrane permeability for paramagnetic

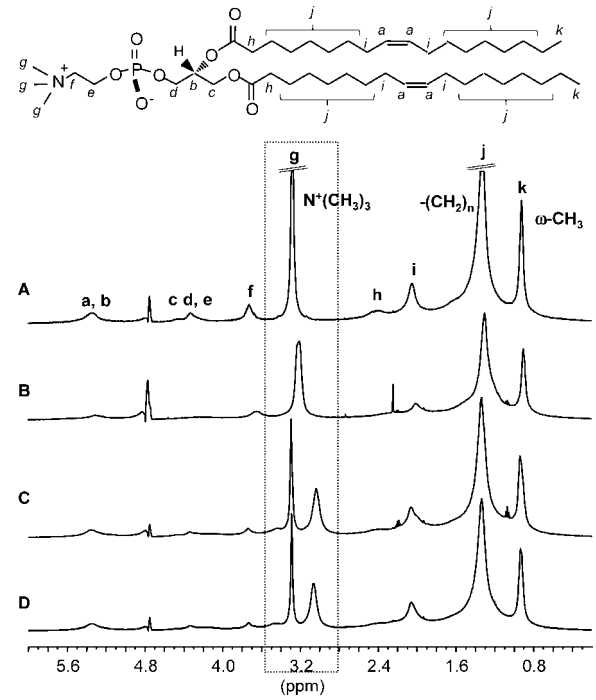

Figure 2. Structure and ^{1}H NMR spectra of 1,2-dioleoyl-*sn*-glycero-3-phosphocholine (DOPC) vesicles (A), DOPC vesicles preloaded with CE (i.e., 1 mM CE and 10 mM DOPC were codissolved in organic solvent (CH_2Cl_2/CH_3OH) before solvent removal, rehydration, and extrusion in PBS) (B), and DOPC vesicles after external addition of CE (C) and MACE (D). All spectra were recorded in PBS (D_2O, pH 7) at a DOPC concentration of 10 mM and molar ratios of CE/DOPC and MACE/DOPC of 0.1 (B−D). The region where choline $-N^+(CH_3)_3$ resonances appear is highlighted.

metal ions was monitored by analyzing temporal changes of inner and outer phospholipid (PL) NMR signals induced by the paramagnetic effect of the nearby metal ions.[21,22] Even though the NMR investigation of kinetics is restricted to slow processes, our studies demonstrate that the NMR spectroscopic approach can provide comprehensive information on the membrane localization and transfer of porphyrinic compounds. The method takes advantage of the large porphyrin ring current effects inducing major shift and line width changes to the NMR signals of PL molecules in spatial proximity. Therefore, evaluating the PL signals allows for deriving rate constants for chlorin distribution within the lipid bilayer. Moreover, NMR can provide not only direct information about time-resolved localization sites of an incorporated compound but also information on the molecular dynamics, for example, motional restrictions conferred to the molecule upon membrane adsorption or aggregation.

In summary, the goals of this study were (i) to determine and compare the membrane distribution of two representative amphiphilic porphyrinic compounds, namely, CE and MACE, (ii) to characterize the kinetics by NMR spectroscopy, and (iii) to determine the factors modulating porphyrin kinetics across the membrane.

Experimental Section

Materials. 1,2-Dioleoyl-*sn*-glycero-3-phosphocholine (18:1 PC (cis); DOPC) was purchased from Avanti Polar Lipids Inc. The cholesterol was obtained from Sigma. Chlorin e6 (CE) and mono-L-aspartyl-chlorin e6 tetrasodium salt (MACE, Npe6) were purchased from Frontier Scientific. The structures of CE and MACE are shown in Figure 1, and the structure of DOPC is shown in Figure 2. The deuterated solvents D_2O (D 99.9%) and NaOD (40% in D_2O, D 99.5%) were obtained from Cambridge Isotopes Laboratories, Inc.

(11) Kuzelova, K.; Brault, D. *Biochemistry* **1994**, *33*, 9447–9459.
(12) Kuzelova, K.; Brault, D. *Biochemistry* **1995**, *34*, 11245–11255.
(13) Maman, N.; Brault, D. *Biochim. Biophys. Acta* **1998**, *1414*, 31–42.
(14) Bonneau, S.; Maman, N.; Brault, D. *Biochim. Biophys. Acta* **2004**, *1661*, 87–96.
(15) Spikes, J. D.; Bommer, J. C. *J. Photochem. Photobiol., B* **1993**, *17*, 135–143.
(16) Voszka, I.; Budai, M.; Szabó, Z.; Maillard, P.; Csík, G.; Gróf, P. *Chem. Phys. Lipids* **2007**, *145*, 63–71.
(17) Csík, G.; Balog, E.; Voszka, I.; Tölgyesi, F.; Oulmi, D.; Maillard, P.; Momenteau, M. *J. Photochem. Photobiol., B* **1998**, *44*, 216–224.
(18) Cruciani, O.; Mannina, L.; Sobolev, A. P.; Cametti, C.; Segre, A. L. *Molecules* **2006**, *11*, 334–344.
(19) Mel'nikov, S. M.; Seijen ten Hoorn, J. W. M.; Eijkelenboom, A. P. A. M. *Chem. Phys. Lipids* **2004**, *127*, 121–141.
(20) Hills, B. P.; Belton, P. S. *J. Magn. Reson.* **1989**, *81*, 227–244.
(21) Nakagawa, H.; Ueno, S.; Okada, S.; Abe, H. *Int. Congr. Ser.* **2007**, *1300*, 311–314.
(22) Degani, H.; Lenkinski, E. *Biochemistry* **1980**, *19*, 3430–3434.
(23) Cabral, D. J.; Small, D. M.; Lilly, H. S.; Hamilton, J. A. *Biochemistry* **1987**, *26*, 1801–1804.
(24) Males, R. G.; Herring, F. G. *Biochim. Biophys. Acta* **1999**, *1416*, 333–338.
(25) Lagoueyte, C.; Subra, G.; Bonnet, P.-A.; Chapat, J.-P.; Debouzy, J.-C.; Fauvelle, F.; Berleur, F.; Roman, V.; Fatome, M.; Fernandez, J.-P. *Eur. J. Pharm. Biopharm.* **1997**, *43*, 73–81.

All chemicals and solvents were used without further purification. CE and MACE stock solutions were freshly prepared in D_2O at a concentration of 15 mM. Chlorin e6 was first transferred into its sodium salt by adding NaOD solution.

Vesicle Preparation. DOPC was dissolved in chloroform. The solvent was then removed by a stream of argon and subsequent evacuation overnight. The resulting phospholipid film was rehydrated with a D_2O-based phosphate buffered saline solution (PBS, 10 mM, pH 7) to yield a phospholipid concentration of 10 mM. The lipid dispersion was vortexed and then submitted to five freeze−thaw cycles. Unilamellar vesicles were obtained from these by extrusion using a 10 mL Lipex Thermobarrel extruder (Northern Lipids Inc.). The lipid dispersion was extruded stepwise through polycarbonate membranes of pore sizes 100, 50, and 30 nm (10 passes through each membrane) in order to obtain homogeneous vesicle sizes. For each series of measurements, fresh DOPC vesicle dispersions were prepared. Vesicle size and size distribution of vesicle preparations were examined by dynamic light scattering (DLS) using a laser diode operated at a wavelength of 785 nm (see the Supporting Information). The DLS data were processed using the ALV-5000 Multiple Tau digital correlator (ALV-Laser GmbH, Langen, Germany). The vesicle preparations exhibited a narrow size distribution with an average hydrodynamic radius (r_H) of 26.8 ± 0.8 nm at neutral pH and were found to be stable over at least 15 days if kept at room temperature (max temporal variation of r_H ± 3.7%). The ratio of DOPC in the outer membrane layer over total DOPC was found to be 0.51 ± 0.03 as determined on a 10 mM DOPC sample in D_2O by ^{1}H NMR spectroscopy using the lanthanide shift reagent $PrCl_3$[26] (see the Supporting Information). To obtain DOPC vesicles containing 10, 20, and 30 mol % cholesterol, the required amounts of DOPC and cholesterol were mixed for each sample in chloroform. From this, vesicles were prepared as described above.

Vesicle Loading with CE and MACE. An amount of 500−600 μL of 10 mM DOPC solution in PBS was transferred to 5 mm NMR tubes (Wilmad), and aliquots of CE or MACE stock solution were added and mixed in the NMR tube to yield the desired molar ratio of CE (MACE)/DOPC. Prior to each series of NMR measurements, the pH of each sample was measured directly in the NMR tube using a pH electrode designed for NMR tubes (Spintrode 180 × 3 mm, Hamilton). The time between mixing of CE or MACE with DOPC vesicles and the first NMR acquisition ("dead time") was about 10 min due to several preparation steps (e.g., pH measurement, matching and tuning of the NMR probe, locking, and shimming procedure).

On a separate set of corresponding samples, the vesicle integrity, size, size distribution, and stability of chlorin loaded vesicles were examined by DLS (see the Supporting Information). The DLS data indicated that chlorin insertion had little effect on vesicle size and size distribution. The average hydrodynamic radii for MACE/DOPC and CE/DOPC at molar ratios of 0.3 and neutral pH were 27.6 ± 0.2 and 26.4 ± 0.4 nm, respectively. The chlorin loaded vesicle preparations were found to retain their narrow size distributions and were stable over at least 15 days at room temperature (max temporal variation of r_H ± 3.7%).

To obtain a sample of 10 mM DOPC vesicles preloaded with CE, defined amounts of DOPC and CE were dissolved in MeOH/CH_2Cl_2 (1:1). After solvent removal, the DOPC/CE mixture was hydrated with PBS, vortexed, and then submitted to freeze−thaw cycles and extrusion as described above.

Nuclear Magnetic Resonance (NMR) Spectroscopy. The NMR experiments were performed on a Bruker DRX-400 spectrometer operating at a ^{1}H resonance frequency of 400.13 MHz. The instrument is equipped with a 5 mm dual probe (BBI) for inverse detection with a z-gradient coil. Some experiments were carried out at elevated temperature (343 K). This is indicated in the text. If not otherwise mentioned, all other measurements were carried out at room temperature (298 K). The ^{1}H NMR spectra were recorded with water presaturation. Typically, 64 transients, a spectral width of 8223 Hz, a data size of 64 K points, an acquisition time of 3.98 s, and a relaxation delay of 4 s were used to acquire the ^{1}H NMR spectra. The free induction decays (FIDs) were signal-averaged, exponentially weighted with a line broadening factor of 1.0 Hz, Fourier-transformed, and phase-corrected to obtain the ^{1}H NMR spectra. Postprocessing of the NMR spectra was performed using the Bruker software 1D WIN−NMR, version 6.0. Fitting procedures were carried out using Origin, version 5.0 (Microcal Software, Inc.). The Levenberg−Marquardt algorithm was applied to minimize the sum of squares. The number of iteration steps was determined by the convergence criterion.

Determination of the Distribution Coefficient of CE and MACE between DOPC Vesicles and the Aqueous Bulk Phase. To determine the distribution coefficient D_{DOPC} for the applied concentration range, solutions of 10 mM DOPC in PBS at pH 7 were titrated with CE and MACE. Likewise, pure PBS was titrated with corresponding amounts of CE and MACE. A ^{1}H NMR spectrum was recorded after each titration step. For each solution, the sums of the chlorin peaks H-5 and H-15 (Figure 1), both in the absence and presence of DOPC vesicles, were integrated. The integrals in pure PBS are directly proportional to the total chlorin concentration $[chl]_{tot}$, while the integrals in the presence of DOPC vesicles correspond to excessive chlorin concentration in the aqueous phase $[chl]_{aq}$ (i.e., not bound to vesicles, since bound chlorin becomes invisible due to strong signal broadening). The concentration of chlorin bound to DOPC vesicles was obtained from the difference $[chl]_{tot} - [chl]_{aq} = [chl]_{DOPC}$. The distribution coefficient was determined according to the equation:

$$D_{DOPC} = \frac{[chl]_{DOPC}/[DOPC]}{[chl]_{aq}/[aq]} \quad (1)$$

With [DOPC] = 0.01 M and [aq] = 55.5 M, that is, [DOPC]/[aq] = 1.8×10^{-4} and $[chl]_{aq} = [chl]_{tot} - [chl]_{DOPC}$, the equation can be rearranged as follows:

$$[chl]_{DOPC} = \frac{(D_{DOPC})(1.8\times10^{-4})}{1+(D_{DOPC})(1.8\times10^{-4})}[chl]_{tot} \quad (2)$$

The distribution coefficient D_{DOPC} can then be obtained from linear regression of $[chl]_{DOPC}$ data points plotted versus $[chl]_{tot}$.

Results

1. ^{1}H NMR Spectrum of DOPC Vesicles in the Presence of CE and MACE. The proton NMR spectrum of DOPC vesicles in PBS is shown in Figure 2A. Resonance assignment of DOPC protons was carried out according to the literature[27] and was confirmed by an ^{1}H−^{1}H COSY experiment. The three major peaks in the DOPC spectrum derive from the choline methyl protons (g, 3.28 ppm), the lipid chain methylene protons (j, 1.33 ppm), and the terminal ω-methyl group (k, 0.92 ppm). Addition of CE (Figure 2C) or MACE (Figure 2D) to DOPC vesicles induces a split of the DOPC $-N^+(CH_3)_3$ resonance and a significant line broadening for the upfield shifted part as is highlighted in Figure 2. In addition, a slight line broadening of all other DOPC peaks (a−f, h−k) occurs as compared to DOPC vesicles in the absence of CE and MACE (Figure 2A). The split of the $-N^+(CH_3)_3$ resonance occurs immediately after mixing of CE or MACE with DOPC vesicles and indicates fast association of the chlorin compounds with the vesicular surface. Therefore, the shifted and broadened portion of the DOPC $-N^+(CH_3)_3$ resonance (3.04 ppm) can be assigned to the outer vesicle monolayer where the porphyrin is located initially, while the nonshifted portion of the DOPC $-N^+(CH_3)_3$ resonance (3.29 ppm) most likely derives from the inner vesicle monolayer initially being devoid of porphyrin. This assumption is supported by the 1:1 integral ratio of the split $-N^+(CH_3)_3$ signals, which

(26) Barsukov, L. I.; Victorov, A. V.; Vasilenko, I. A.; Evstigneeva, R. P.; Bergelson, L. D. *Biochim. Biophys. Acta* **1980**, *598*, 153–168.

(27) Veatch, S. L.; Polozov, I. V.; Gawrisch, K.; Keller, S. L. *Biophys. J.* **2004**, *86*, 2910–2922.

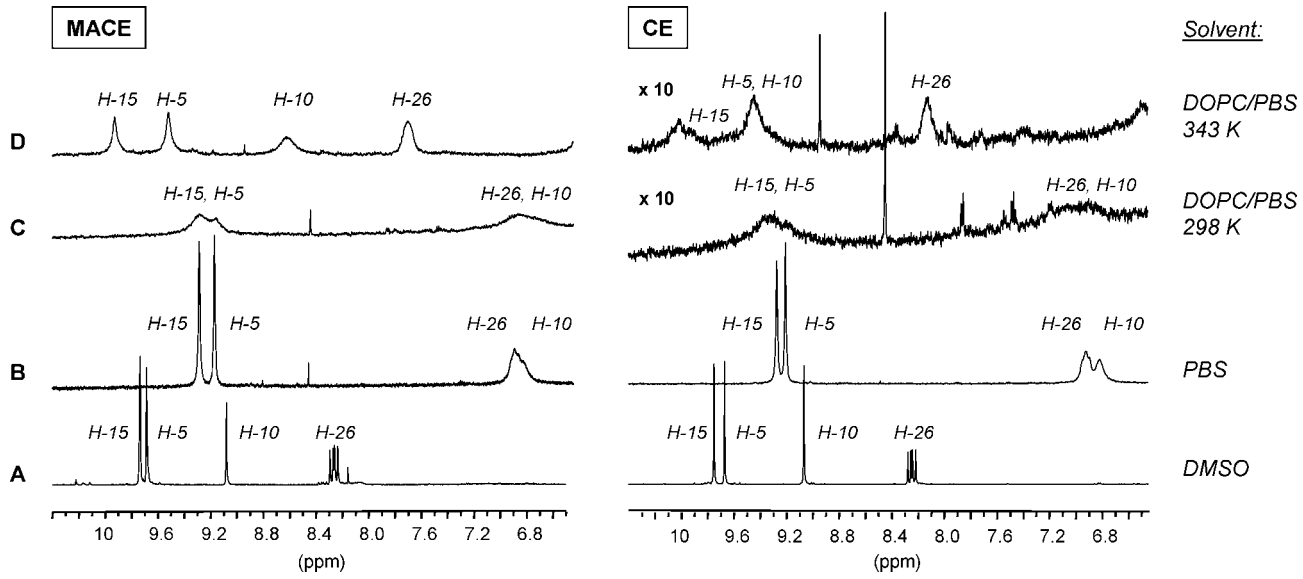

Figure 3. Aromatic region of ^{1}H NMR spectra of MACE (left) and CE (right): 15 mM in DMSO-d_6 (A), 2.5 mM in PBS (D_2O, pH 7) (B), 2.5 mM after addition to DOPC vesicles (10 mM in PBS, pH 7) at 298 K (C), and at 343 K (D). The signals were assigned to the mesoprotons H-15, H-5, and H-10 and to the vinyl proton H-26 (see Figure 1). The strong upfield shift of the resonances H-26 and H-10 in (B) compared to (A) indicates the presence of oligomers in PBS.

corresponds to the quantitative distribution of PL molecules found for the outer and inner membrane layers of pure DOPC vesicles using the lanthanide shift reagent praseodym (see the Experimental Section and Supporting Information). Furthermore, no split choline signal occurs in the case of preloaded CE/DOPC vesicles (Figure 2B). To yield such vesicles, CE and DOPC were mixed in *organic solvent* (CH_3OH/CH_2Cl_2) where DOPC is *monomeric*, before the solvent was removed, and the CE/DOPC vesicles were prepared in PBS and extruded. The aim of this experiment was to show the difference between *external addition* of CE to prepared vesicles versus *preloading* of vesicles with CE. As is shown in Figure 2B, if preloaded with CE, the DOPC $-N^+(CH_3)_3$ peak is not split into two parts but is shifted and broadened as compared to DOPC vesicles in the absence of chlorin (Figure 2A). This is most likely due to the close proximity of the porphyrinic compound with both inner *and* outer $-N^+(CH_3)_3$ groups. The small sharp peaks in Figure 2B and C derive from residual solvent (2.2 ppm) and from an impurity accompanying CE as it is obtained in its commercial form (multiplets at 1.0 and 2.17 ppm), but obviously this does not interfere with the investigated system.

2. Aggregation Behavior of CE and MACE. The aggregation state of porphyrinic molecules is assumed to be relevant for their efficiency in PDT.[1] In order to investigate the aggregation state in the absence and presence of DOPC vesicles, the ^{1}H NMR spectra of CE and MACE in DMSO-d_6, in pure PBS (D_2O), and in DOPC/PBS solution were compared (Figure 3).

2.1. Chlorin ^{1}H NMR Signals in DMSO and PBS (D_2O). For MACE, it has been suggested that it is present as free monomers in dimethyl sulfoxide (DMSO), while oligomers are formed in aqueous solution.[28] Oligomerization is indicated by characteristic "unusual" shift changes and signal broadening of certain protons, for example, the meso proton in position 10 (Figure 1).[28] Such indications for an oligomerization could be found for both CE and MACE in PBS by our NMR spectroscopic investigations for the full investigated concentration range ($0.13-15 \times 10^{-3}$M). This is demonstrated in Figure 3 by comparing the aromatic regions of the ^{1}H NMR spectra of CE and MACE in DMSO (A) and PBS (B), both acquired in the absence of vesicles. The resonances shown in Figure 3 were assigned to the meso protons H-15, H-5, and H-10, and to the vinyl proton H-26.[28] The significant upfield shift and line broadening in PBS compared to DMSO of the signals assigned to H-10 and H-26 (Figure 3 B) suggest the presence of di- or oligomers for both CE and MACE in PBS.

2.2. Chlorin ^{1}H NMR Signals in the Presence of Vesicles. Two PBS samples, each containing the same total chlorin concentration (2.5×10^{-3}M), one in the absence (Figure 3B) and the other in the presence of vesicles (Figure 3C), were compared. In the presence of DOPC vesicles, CE and MACE resonance positions still suggest the presence of aggregates; however, the signals are significantly further broadened (Figure 3C). For quantitative comparison, the summed integrals of chlorin H-5 and H-15 signals were determined. In the presence of vesicles, the integrals which are proportional to chlorin concentration were clearly reduced and only yielded a fractional amount of the integrals obtained in pure PBS (about 25% of total CE and 60% of total MACE). Thus, in the presence of vesicles, the chlorin signals most likely account for excessive aggregated chlorin *not bound to the vesicle*, while the signals of the chlorin portion incorporating into the vesicles become "NMR invisible" due to strong signal broadening. This interpretation is also supported by the following finding: Heating the sample up to 343 K resulted in signal narrowing and nonuniform downfield shifts of the chlorin signals assigned to the meso protons H-15, H-5, and H-10, and to H-26 toward the shift positions of the monomer form, indicating dissociation of the chlorin aggregates in the aqueous bulk phase (Figure 3D). However, no additional signals occur in the aromatic region and the integrals remain approximately unchanged at 343 K compared to those determined at 298 K. Thus, the signals in the aromatic region clearly derive from "free" chlorin in the aqueous phase, while the vesicle-associated fraction of CE and MACE is not released from the vesicles and seems to remain "NMR- invisible" even at elevated temperature.

3. Binding of CE and MACE to DOPC Vesicles. In Figure 4, the concentration of chlorin (CE or MACE) bound to DOPC

(28) Gomi, S.; Nishizuka, T.; Ushiroda, O.; Uchida, N.; Takahashi, H.; Sumi, S. *Heterocycles* **1998**, *48*, 2231–2243.

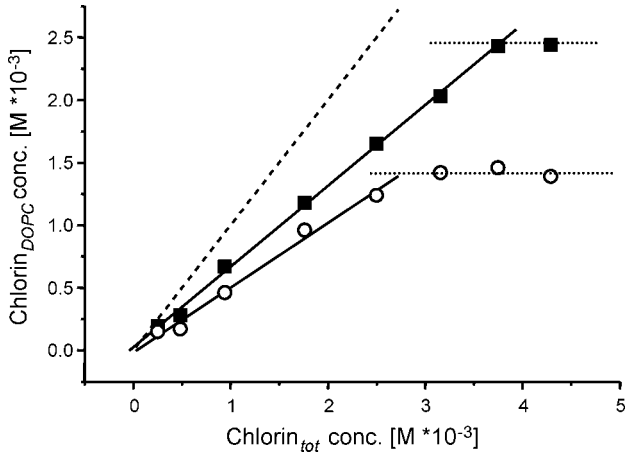

Figure 4. Plot of chlorin concentration bound to DOPC versus total chlorin concentration for CE (■) and MACE (○) added to 10 mM DOPC in PBS (pH = 7.10 ± 0.05). Solid lines correspond to linear regression of data points below saturation of DOPC with chlorin (dotted lines correspond to saturation) to derive the distribution coefficients (see Experimental Section). The dashed line corresponds to the theoretical case of complete uptake of chlorin by the DOPC vesicles.

vesicles $[chl]_{DOPC}$ was plotted as a function of total chlorin concentration added to a 10×10^{-3} M DOPC solution $[chl]_{tot}$. Above a certain total chlorin concentration, values for $[chl]_{DOPC}$ remain constant, indicating vesicle saturation. Linear regression of the data points below vesicle saturation yielded the distribution coefficient for the applied concentration range which was found to be $D_{DOPC} = (10 \pm 0.6) \times 10^3$ for CE and $D_{DOPC} = (6 \pm 0.8) \times 10^3$ for MACE. These distribution coefficients actually refer to the DOPC molecules from the outer monolayer only, which accounted for about 50% of total DOPC. The dashed line in Figure 4 corresponds to the theoretical case that all chlorin added to the vesicle solution would be bound to DOPC vesicles. Thus, the deviation from this theoretical line, that is, the distribution coefficient D_{DOPC} for CE and MACE, has to be taken into account in the following where data are reported with respect to total chlorin concentration added to the vesicle solutions or molar ratios of total chlorin over DOPC concentration.

The plot also demonstrates the limited capacity for CE and MACE taken up by the outer vesicle layer: Above a threshold, increases in $[chl]_{tot}$ do not further increase $[chl]_{DOPC}$. Saturation of the vesicles (10×10^{-3} M DOPC) is reached approximately at a total chlorin concentration of 3.7×10^{-3} M for CE and 2.7×10^{-3} M for MACE.

4. Kinetics of Chlorin Distribution within the Membrane. To study the kinetics of chlorin distribution within the model membrane, spectra of DOPC vesicles in neutral PBS (pH 7.1) were recorded repeatedly after addition of CE and MACE over a time period of approximately 300 h. In Figure 5, the time-dependent changes of the ^{1}H NMR spectra of the vesicles after the addition of CE at molar ratios CE/DOPC of 0.025 (A) and 0.3 (B) and after the addition of MACE at a molar ratio MACE/DOPC of 0.3 (C) are shown for the spectral region where the split $-N^+(CH_3)_3$ peaks occur. Significant differences in the time-dependent behavior of equal molar amounts of CE and MACE at the model membrane were found: In the presence of MACE, the signal positions of the split DOPC choline resonances remained essentially unchanged, indicating that MACE presumably remains attached to the membrane surface without crossing the lipid bilayer. In contrast, in the presence of CE, a temporal converging of the split choline signals (labeled "inner" and "outer" in Figure 5) was observed, suggesting slow distribution of CE across the phospholipid bilayer. Moreover, for CE/DOPC = 0.3, the inner choline signal exhibits significant temporal broadening. At both CE concentrations, the shift difference between the inner and outer $-N^+(CH_3)_3$ choline resonances decreases over time, indicating equilibration of CE between the two membrane layers. However, while at low molar ratio CE/DOPC of 0.025 (Figure 5A), the split choline signals completely merge, at high molar ratio CE/DOPC of 0.3 (Figure 5B) the two signals remain separated in the investigated time period. In Figure 6, the corresponding chemical shift δ of the inner and outer methyl choline signals in the presence of CE and MACE is plotted as a function of time (upper row). Chemical shift changes of the inner methyl choline signal in the presence of CE could be simplest modeled in the first approximation by a single exponential decay for both low and high CE concentration (Figure 6A and B), resulting in rate constants of 0.18×10^{-5} and 0.5×10^{-5} s^{-1}, respectively. For CE/DOPC = 0.025 (Figure 6A), the corresponding *outer* methyl choline signal continuously moves downfield toward the inner methyl choline signal, while for CE/DOPC = 0.3 (Figure 6B) it initially moves slightly upfield until it reverses after about 25 h, and then it shifs downfield. In Figure 6, bottom row, the line widths of the inner and outer N-methyl choline resonances are shown as function of time after addition of MACE and CE. Since, at low CE concentration, the split choline signals were not completely separated, line widths were not evaluated in this case.

Integral ratios for the outer and inner methyl choline resonances remained more or less unchanged for the investigated time span in the presence of both CE (integral ratio = 0.99 ± 0.06) and MACE (0.97 ± 0.02), indicating constant equal distribution of DOPC in both membrane layers.

Besides the above-described distinct upfield shift of the N-methyl choline resonance upon MACE and CE adsorption to the outer monolayer, the shifted portion of this signal (i.e., the outer choline signals) also experiences a strong line broadening from about 12 Hz in the absence of chlorin to 41 and 58 Hz immediately after addition of MACE and CE, respectively. For addition of MACE, the outer N-methyl choline resonance narrows in the temporal course to about 25 Hz while the inner N-methyl choline signal remains more or less unchanged (Figure 6). Thus, despite the lack of obvious membrane translocation of MACE, a slow process occurs which seems to be restricted to the outer membrane layer. However, and in strong contrast to MACE, after addition of equal amounts of CE, the line width of the inner $-N^+(CH_3)_3$ signal exhibits a prominent time course proceeding through a maximum value before leveling off at a line width of about 38 Hz. The line width of the outer $-N^+(CH_3)_3$ signal on the other hand decreases exponentially with a rate constant of 1.22×10^{-5} s^{-1} to a limiting value of about 32 Hz. Accordingly, in addition to the temporal chemical shift changes, signal broadening for the inner and concomitant signal narrowing for the outer $-N^+(CH_3)_3$ group as function of time are likewise indicative for chlorin distribution between the two membrane layers.

For the ^{1}H resonances of the DOPC *acyl chain protons*, similar but less pronounced temporal chemical shift changes as for the inner $-N^+(CH_3)_3$ signal could be obtained after addition of MACE and CE. This is shown in Figure 7 for a molar ratio of chlorin/DOPC of 0.3. While for MACE no significant changes were observed, for CE $\delta((CH_2)_n)$ and $\delta(\omega\text{-}CH_3)$ decay exponentially over time, resulting in rate constants of 0.8×10^{-5} s^{-1} for both signals, that is, similar to the value obtained from the inner choline signal (0.5×10^{-5} s^{-1}). Unlike the $-N^+(CH_3)_3$ signals, the inherently broader line widths of the acyl chain signals exhibited only minor changes over the investigated time range.

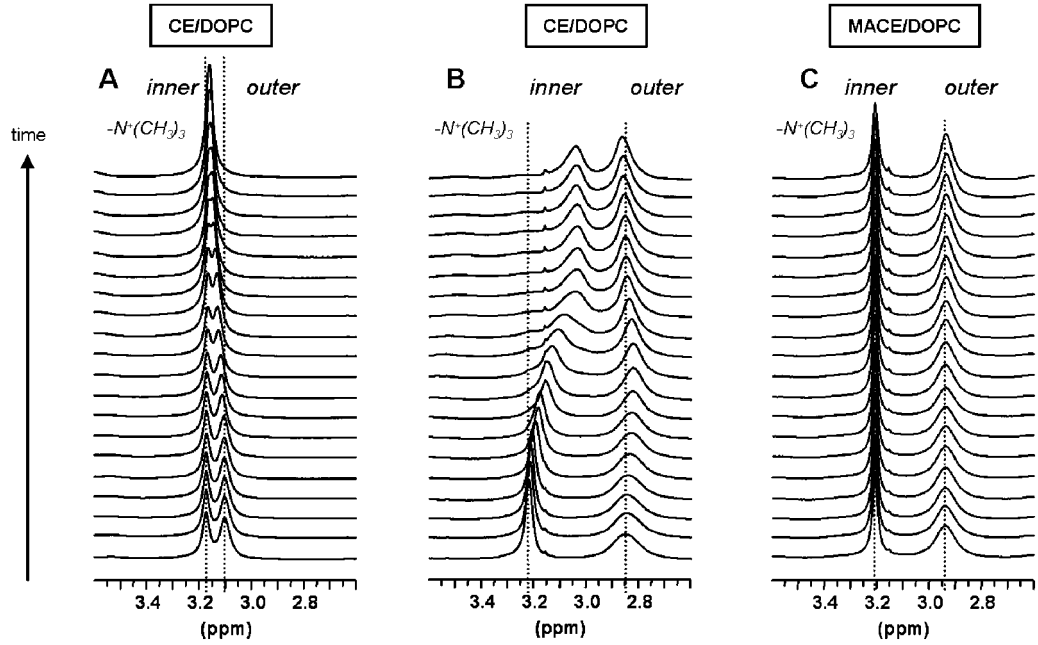

Figure 5. ^{1}H NMR spectra of split inner and outer DOPC choline $-N^+(CH_3)_3$ resonances as observed over time (0−300 h, from bottom to top, time scale not linear) after addition of different amounts of CE (A, B) and MACE (C) to 10 mM DOPC vesicle solution in PBS (D_2O, pH 7.1). Molar ratios: CE/DOPC = 0.025 (A), CE/DOPC = 0.3 (B), and MACE/DOPC = 0.3 (C). Converging of inner and outer choline signals in (A) and (B) indicate equilibration of CE between the membrane layers.

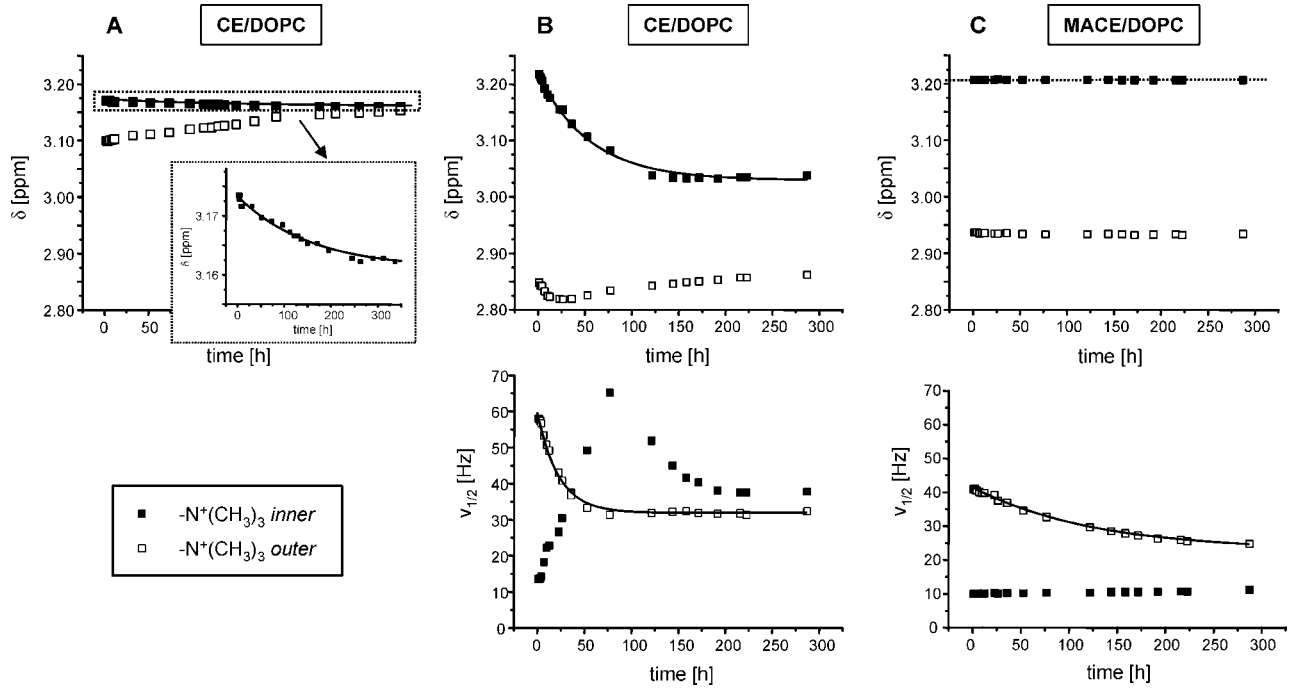

Figure 6. Plots of chemical shift δ (upper row) and line width $\nu_{1/2}$ (bottom row) of inner (solid symbols) and outer (open symbols) DOPC choline $-N^+(CH_3)_3$ resonances versus time after addition of CE (A, B) and MACE (C) to 10 mM DOPC/PBS (pH 7.1). Molar ratios: CE/DOPC = 0.025 (A), CE/DOPC = 0.3 (B), and MACE/DOPC = 0.3 (C). Solid lines correspond to data fitting to an exponential decay function.

5. Concentration-Dependence of CE Transition across the DOPC Bilayer. In Figure 8A, the chemical shift difference of the split inner and outer methyl choline groups $\Delta\delta = \delta$ ($-N^+(CH_3)_3$ *inner*) $- \delta$ ($-N^+(CH_3)_3$ *outer*) immediately after addition of CE or MACE is plotted as function of total added concentration of CE and MACE, respectively. The plots exhibit an asymptotic correlation between the initial split of methyl choline signals $\Delta\delta$ and chlorin concentration. The continuity of the changes in $\Delta\delta$ also indicates that there is no abrupt conformation change of the vesicles.

To probe the effect of CE concentration or molar ratio CE/DOPC on the CE transfer kinetics across the bilayer membrane, time-dependent spectra were acquired at various CE concentrations ($0.25-4.3 \times 10^{-3}$ M) and constant DOPC concentration (10×10^{-3} M, molar ratios CE/DOPC 0.025−0.6, pH = 7.10 ± 0.05). As was already evident from the spectra shown in Figure

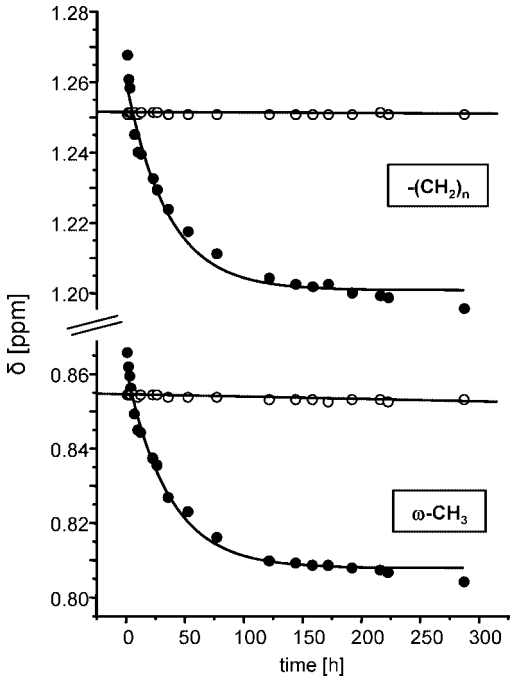

Figure 7. Plots of chemical shifts δ of the DOPC acyl chain $-(CH_2)_n$ and ω-CH_3 resonances versus time after addition of CE (solid symbols) and MACE (open symbols) to 10 mM DOPC/PBS (pH 7.1). Molar ratios: CE/DOPC and MACE/DOPC = 0.3. Lines correspond to fitting of the data to an exponential decay (for CE) and linear (for MACE) function.

5A and B, the inner and outer choline signals did not merge at equilibrium for higher CE concentration as opposed to a low molar ratio CE/DOPC = 0.025. In Figure 8B, $\Delta\delta$ of the split choline signals is plotted as a function of total added CE concentration at time $t = 0$ (i.e., immediately after CE addition) and at equilibrium. The arrows indicate converging of the split choline signals over time. The remaining chemical shift difference $\Delta\delta$ of the split choline signals at equilibrium was found to increase with total CE concentration. While at a concentration of 0.25×10^{-3} M (CE/DOPC = 0.025) the $\Delta\delta$ values decayed to zero, an increasing shift difference $\Delta\delta$ remained at higher CE concentrations (molar ratios of 0.1−0.6). For each CE concentration, for which the membrane transition rates were investigated, the half-life $t_{1/2}$ was determined graphically from the plots of chemical shift versus time for the single DOPC resonances $-N^+(CH_3)_{3,\text{inner}}$, $-(CH_2)_n$, and ω-CH_3. $t_{1/2}$ is defined as the time at which the chemical shift change ($\Delta\delta$) has reached 50% ($\Delta_{50\%}\delta$) of its maximum deviation ($\Delta_{max}\delta$) from δ at time $t = 0$. This graphical determination of $t_{1/2}$ was selected instead of the determination of rate constants by fitting the data points as above (see section 4) because it is a model-independent parameter and single exponential decay could not be assumed for all concentrations and peaks. In Figure 9A, the reciprocal half-life $t_{1/2}^{-1}$ as function of CE concentration in the vesicular phase is shown. Values of $t_{1/2}^{-1}$ increase with increasing CE concentration. Averaging the data points obtained for the three different DOPC peaks at each CE concentration, CE partitions with an average half-life of 108, 32, 23, and 17 h corresponding to molar ratios CE/DOPC of 0.025, 0.1, 0.3, and 0.6, respectively.

6. Effect of Membrane Rigidity on CE Transition across the DOPC Bilayer. To probe the effect of membrane rigidity on the transition rate of CE across the DOPC bilayer, DOPC vesicles were prepared containing various amounts of cholesterol (10, 20, and 30 mol %), which is well-known to reduce the mobility of PL molecules in the bilayer.[19] Time-dependent ^{1}H NMR spectra were recorded for these samples after addition of CE at a molar ratio of 0.3, neutral pH, and equal DOPC concentration. Peak integrals of CE H-15 and H-5 protons, assigned to CE from the aqueous phase, were slightly reduced with increasing cholesterol content in the membrane, indicating enhanced uptake of CE into the vesicular phase. In analogy to Figure 9A, the half-life $t_{1/2}$ was determined from the single DOPC resonances $-N^+(CH_3)_{3,\text{inner}}$, $-(CH_2)_n$, and ω-CH_3 by plotting the corresponding chemical shift versus time for each cholesterol concentration. In Figure 9B, the reciprocal half-life $t_{1/2}^{-1}$ as a function of mol % cholesterol in 10×10^{-3} M DOPC vesicle solution is shown. Values of $t_{1/2}^{-1}$ decrease strongly and exponentially with increasing cholesterol content in the membrane. Thus, CE distribution across the PL bilayer is slowed down at, for example, 30 mol % cholesterol to an average half-life of $t_{1/2} = 88$ h as compared to an average half-life of $t_{1/2} = 26.5$ h for cholesterol-free membranes.

Discussion

This study clearly shows for the example of CE and MACE that distribution processes of porphyrins between the outer and inner phospholipid monolayers of model membranes can be effectively monitored by ^{1}H NMR spectroscopy through analysis of chemical shifts and line widths of vesicle resonances. Upon addition of porphyrins, close proximity of the porphyrinic compound changes the ^{1}H spectra of the vesicles significantly, allowing for separate analysis of inner and outer vesicle layers. Kinetic parameters for the transition across the DOPC bilayer such as half-lives and rate constants were determined. In comparison to CE, MACE transbilayer movement was significantly reduced, with MACE remaining more or less attached to the outer membrane layer only. This demonstrates the strong influence of the porphyrin structure on the distribution process. A positive correlation was found between transfer rate and molar ratio CE/DOPC. Enhanced membrane rigidity induced by increasing amounts of cholesterol into the model membrane led to a decrease of CE transfer rates across the membrane.

1. Qualitative Changes in the ^{1}H NMR Spectrum of DOPC Vesicles upon Chlorin Addition. The addition of both CE and MACE to DOPC vesicles resulted in a clear split of the $-N^+(CH_3)_3$ resonance into two resolved peaks (Figure 2C and D). This distinct upfield shift of the outer N-methyl resonance is presumably caused by the porphyrin ring current of the chlorin macrocycle being in close proximity to the polar head region of the outer phospholipid monolayer. Similarly, a split of the N-methyl choline resonance[29−31] or shifts of other lipid protons[32−34] upon insertion of aromatic amphiphilic compounds into model membranes have been attributed to the short-range ring current effect induced by the adjacent drug molecules. Owing to the observed N-methyl choline shift separation in our study, the two monolayers can thus be well distinguished as long as no fast, immediate distribution of the inserted drug between the two layers occurs. However, if CE is mixed with DOPC *monomers in organic solvent* and if from this mixture vesicles are prepared after solvent removal and rehydration, CE is enabled to distribute evenly between the inner and outer PL monolayer from the beginning. Thus, the PL molecules in both monolayers are equally

(29) Eriksson, L. E. G. *Biophys. Chem.* **1987**, *26*, 9–18.
(30) Jones, G. P.; Paleg, L. G. *Biochemistry* **1984**, *23*, 1521–1524.
(31) Różycka-Roszak, B.; Przyczyna, A.; Pernak, A. *Biophys. Chem.* **2004**, *109*, 271–279.
(32) Fraceto, L. F.; Spisni, A.; Schreier, S.; de Paula, E. *Biophys. Chem.* **2005**, *115*, 11–18.
(33) Colley, C. M.; Metcalfe, J. C. *FEBS Lett.* **1972**, *24*, 241–246.
(34) Kuroda, Y.; Kitamura, K. *J. Am. Chem. Soc.* **1984**, *106*, 1–6.

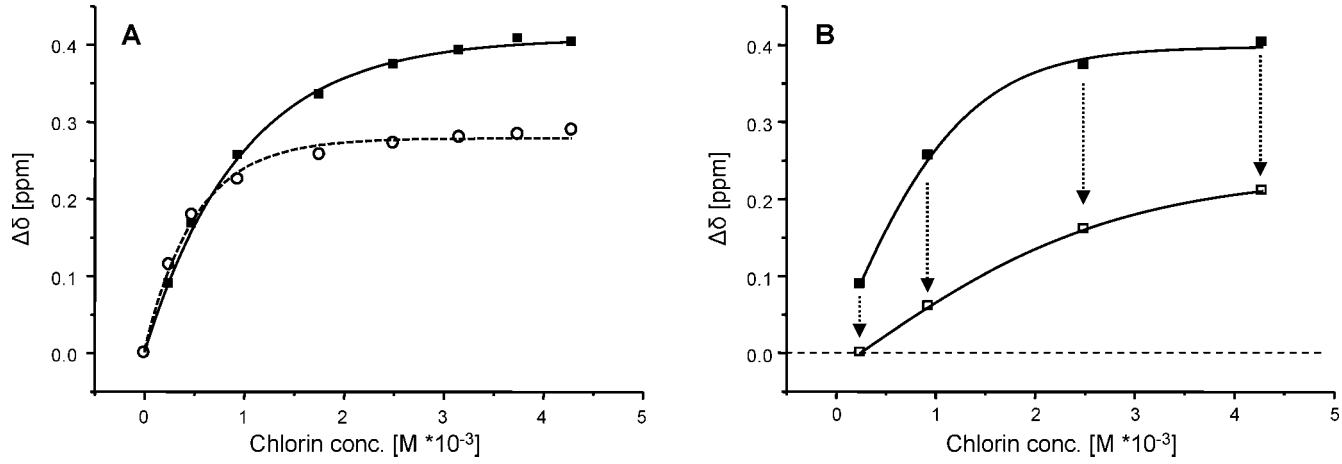

Figure 8. Chemical shift difference $\Delta\delta$ of DOPC inner and outer choline $-N^+(CH_3)_3$ signals after chlorin addition to 10 mM DOPC/PBS as function of total CE and MACE concentration, respectively (pH = 7.10 ± 0.05). (A) $\Delta\delta$ at time $t = 0$, that is, immediately after addition of CE (■) and MACE (○); (B) $\Delta\delta$ after addition of CE at time $t = 0$ (■) and at equilibrium (□). The arrows indicate temporal converging of the split choline signals. Lines correspond to fitting of the data to an asymptotic function.

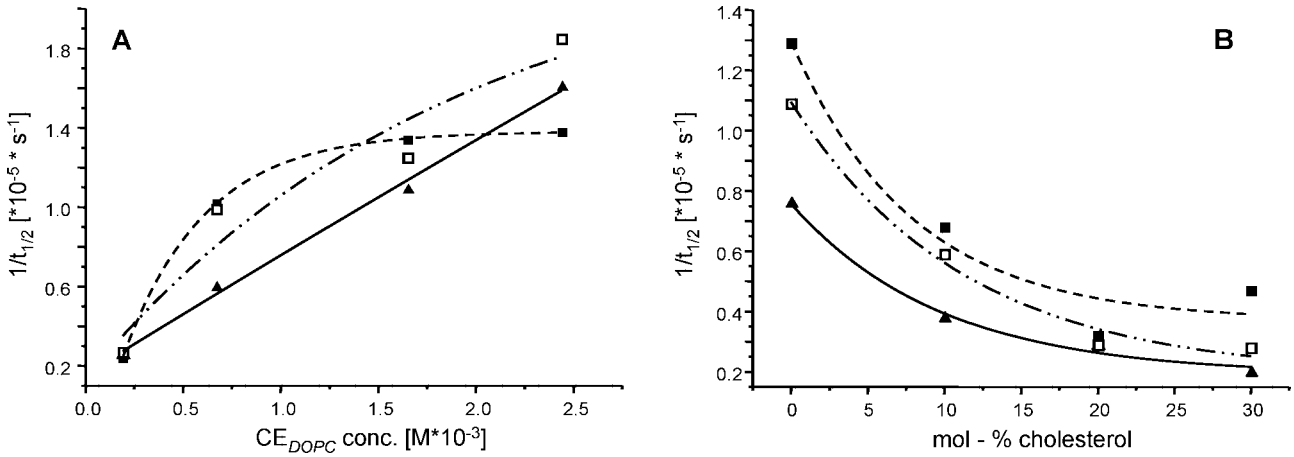

Figure 9. Reciprocal half-life ($1/t_{1/2}$) as determined from plots of δ [ppm] versus time for DOPC inner choline $-N^+(CH_3)_3$ (▲), $-(CH_2)_n$ (■), and ω-CH_3 (□) resonances ([DOPC] = 10 mM, pH = 7.10 ± 0.05). (A) $1/t_{1/2}$ as function of CE concentration in the DOPC vesicular phase; (B) $1/t_{1/2}$ as function of cholesterol content in 10 mM DOPC vesicle solution at molar ratio CE/DOPC = 0.3. Lines correspond to fitting of the data (A) to an asymptotic function and (B) to an exponential decay function.

exposed to CE, obtaining equal chemical surroundings, and cannot be distinguished in the NMR spectrum anymore (Figure 2B).

Line broadening of DOPC signals upon CE or MACE insertion seems to be mainly due to (i) a decrease in mobility of the PL molecules, for example, restricted conformational isomerization and restricted librational motions, that is, oscillating-like motions within the membrane,[35] and (ii) the influence of chemical shift anisotropy (CSA) on DOPC protons induced by neighboring chlorin molecules. Both factors affect the relaxation behavior of the DOPC protons and in turn their signal line width.[36] An increase in vesicle size causing decreased vesicle tumbling would also result in line broadening, although this would affect all DOPC resonances to the same extent. Moreover, dynamic light scattering measurements indicated that the vesicle size did not change significantly upon either CE or MACE insertion.

2. Aggregation of CE and MACE. Porphyrinic compounds with an amphiphilic structure such as CE and MACE tend to self-associate in aqueous solution.[37] This tendency, the aggregate structure, and size depend on factors such as the nature of the polar side chains, the pH of the surrounding medium, and the stereochemistry of the porphyrin molecule.[37−39] The study of porphyrin aggregation by ^{1}H NMR spectroscopic investigations analyzing ring current induced shifts has been well documented by the work of Abraham et al.[40,41] As was derived from their ^{1}H NMR spectra, both CE and MACE are monomeric in DMSO, showing sharp peaks throughout (Figure 3A), but self-associate in aqueous PBS solution, most likely forming small oligomers which still give rise to sharp peaks for H-5 and H-15 (Figure 3B). The characteristic upfield shifts and line broadening of H-10 and the vinyl proton H-26 in PBS are most likely induced by the ring current of neighboring chlorin molecules forming the aggregate (Figure 3).[28,40,41] In pure PBS, no other but intermolecular interactions between self-associating chlorin molecules may account for the effects observed. In addition, the temperature effect, that is, disaggregation upon heating, is typical for aggregate

(35) Huster, D.; Arnold, K.; Gawrisch, K. *J. Phys. Chem. B* **1999**, *103*, 243–251.
(36) Calzolai, L.; Gaggelli, E.; Maccotta, A.; Valensin, G. *J. Magn. Reson., Ser. B* **1996**, *112*, 228–235.
(37) Kadish, K. M., Smith, K. M., Guilard, R., Eds. *The Porphyrin Handbook*; Academic Press: New York, 2000; Vol. *5*, pp 46−50.
(38) Brown, S. B.; Shillock, M.; Jones, P. *Biochem. J.* **1976**, *153*, 279–285.
(39) Aggarwal, L. P. F.; Borissevitch, I. E. *Spectrochim. Acta* **2006**, *63A*, 227–233.
(40) Abraham, R. J.; Smith, K. M.; Goff, D. A.; Lai, J. *J. Am. Chem. Soc.* **1982**, *104*, 4332–4337.
(41) Abraham, R. J.; Smith, K. M. *J. Am. Chem. Soc.* **1983**, *105*, 5734–5741.

formation via hydrophobic interactions in polar solvents[42] and further supports the existence of aggregates.

The chlorin signals in the presence of vesicles (Figure 3C) were assigned to excessive chlorin in the aqueous bulk phase not associated to vesicles. The lack of signals deriving from chlorin in the vesicular phase is most likely due to strong line broadening caused by restricted mobility of the intercalated chlorin molecules. Similarly, NMR visibility of resolved cholesterol proton signals was diminished in the ^{1}H spectra of the cholesterol containing DOPC vesicles. In agreement with this, lack of ^{1}H NMR signal detection has been reported not just for cholesterol[43−45] but also for porphyrins[44] and peptides[46] located in PL bilayers. The additional line broadening of resonances from excessive chlorin in the aqueous phase in the presence of vesicles may be caused by formation of *larger aggregates* which exhibit *reduced tumbling and shortened relaxation time*. Signal broadening may also be due to slow exchange of chlorin between the aqueous and the vesicular phase. However, quantification and heating both indicate that the chlorin signals in the presence of vesicles represent only a fraction of the total chlorin amount added to the vesicle solution. Only this fraction is accessible toward temperature induced disaggregation (Figure 3C, D). Thus, the formation of larger aggregates potentially triggered by the presence of vesicles is more likely to be the cause for further signal broadening in the presence of DOPC vesicles.

Due to the lack of chlorin signals from the vesicular phase, it cannot be derived from the NMR spectra whether CE and MACE incorporate as monomers or as oligomers into the vesicles. Previous studies have shown that porphyrins incorporate into micellar phases as monomers[47] and that porphyrin aggregates can be broken up by inserting them into cyclodextrins[48] or PL micelles (own unpublished results). For MACE, an aggregate structure formed by shifted stacks of two chlorin molecules has been proposed with the carboxylic side chains of each molecule at the periphery pointing in opposite directions.[28] However, such a dimerization would be unfavorable for membrane intercalation into vesicles, since it cancels the cooperative asymmetry properties of the porphyrin molecule.[14]

3. Binding of CE and MACE to DOPC Vesicles. Saturation of the outer DOPC vesicle layer with either CE or MACE was determined from the plot of vesicle-bound versus total chlorin concentration (Figure 4). The figure may suggest that for MACE a plateau is reached at lower concentrations, indicating that binding sites at the outer vesicle layer may be saturated at a somewhat lower concentration for MACE than for CE, which might be attributed to the higher number of carboxylate groups in MACE. More clearly, however, the plot demonstrates that also below this saturation not all chlorin added to the vesicle solution partitions into the vesicular phase. The coefficient for CE and MACE distribution between the aqueous and vesicular phase encompassing both protonated and deprotonated forms could be determined quite accurately for the investigated concentration range from linear regression of the data points below saturation. However, for CE, the D_{DOPC} value of $(10 \pm 0.6) \times 10^3$ as determined by our NMR experiments is smaller compared to that for CE partitioning into DOPC vesicles as determined by fluorescence measurements at neutral pH reported in the literature.[49] This discrepancy is most likely due to the large difference in the applied concentration ranges. The actual chlorin concentrations in the lipid bilayer may influence the uptake of further chlorin molecules into the membrane, and membrane packing densities can influence the membrane partitioning of a given compound.[50] Accordingly, the membrane−water partition coefficient of a detergent into POPC vesicles was found to decrease rapidly with increasing molar detergent/membrane ratios.[51] Thus, the high membrane affinity found for CE and MACE in our experimental setup may even be higher at low concentrations. The D_{DOPC} value of CE ($(10 \pm 0.6) \times 10^3$) was found to be higher than that for MACE ($(6 \pm 0.8) \times 10^3$). This difference correlates with the difference in polarity of the two chlorin compounds with CE being more hydrophobic than MACE, which bears one more carboxylate group at its side chains. While amphiphilicity seems to be a prerequisite to partition into the membrane, the intramolecular hydrophilicity−hydrophobicity balance seems to be crucial for the membrane partition coefficient besides the aggregation behavior. Accordingly, Wiehe et al. have shown in a systematic study of porphyrinic compounds that membrane affinity can be fine-tuned by modulating this intramolecular balance.[52]

4. Kinetics of Transfer across the Membrane. *4.1. Parameters for Deriving Information on Kinetics.* Since both upfield shift and presumably also line broadening of DOPC signals depend on chlorin proximity and are therefore sensitive markers for the amount of chlorin taken up, the temporal changes of the DOPC inner $-N^+(CH_3)_3$ and the $-(CH_2)_n$ and ω-CH_3 signals in the presence of CE allow one to monitor the transbilayer movement of CE. While the *outer* membrane layer takes up CE or MACE immediately after addition of the chlorin compounds, the initial concentration of chlorin in the *inner* membrane layer is assumed to be close to zero, which is confirmed by the unchanged chemical shift of the inner choline resonance. Due to transbilayer distribution of CE, temporal changes in the resonance position of the inner methyl choline group are observed (Figure 6). Therefore, the chemical shift of this signal can be evaluated for assessing the kinetics of transbilayer movement. Average resonance positions of the unresolved inner and outer lipid chain methylene–$(CH_2)_n$ and terminal methyl group ω-CH_3 protons experienced similar, coherent changes as observed for the inner choline methyl group (Figure 7). Therefore, these lipid chain signals ($-(CH_2)_n$ and ω-CH_3) could likewise be evaluated for determining rate constants (Figure 7) or half-lives of CE transbilayer movement (Figure 9).

In addition to chemical shift, the line widths of the inner and outer $-N^+(CH_3)_3$ signals exhibit pronounced temporal changes (Figure 6). Following the initial split and line broadening of the outer methyl choline resonance upon CE addition, the line width of the outer methyl choline signal ($\nu_{1/2,outer}$) decreases continuously while simultaneously the line width of the inner methyl choline signal ($\nu_{1/2,inner}$) increases and passes through a maximum. Both time courses can most likely be attributed to CE transbilayer distribution. However, values for $\nu_{1/2,outer}$ decay with a slightly higher rate constant ($k = 1.22 \times 10^{-5}$ s^{-1}) as compared to the temporal chemical shift changes of the inner methyl choline

(42) Rubires, R.; Crusats, J.; El-Hachemi, Z.; Jaramillo, T.; Lopez, M.; Valls, E.; Farrera, J.-A.; Ribo, J. M. *New J. Chem.* **1999**, *23*, 189–198.
(43) Holland, G. P.; Alam, T. M. *J. Magn. Reson.* **2006**, *181*, 316–326.
(44) Da Costa, G.; Chevance, S.; Le Rumeur, E.; Bondon, A. *Biophys. J.* **2006**, *90*, L55–L57.
(45) Da Costa, G.; Mouret, L.; Chevance, S.; Le Rumeur, E.; Bondon, A. *Eur. Biophys. J.* **2007**, *36*, 933–942.
(46) Ciobanu, L.; Rubakhin, S. S.; Stuart, J. N.; Fuller, R. R.; Webb, A. G.; Sweedler, J. V. *Anal. Chem.* **2004**, *76*, 2331–2335.
(47) Vermathen, M.; Louie, E. A.; Chodosh, A. B.; Ried, S.; Simonis, U. *Langmuir* **2000**, *16*, 210–221.
(48) Ribó, J. M.; Farrera, J.-A.; Valero, M. L.; Virgili, A. *Tetrahedron* **1995**, *51*, 3705–3712.
(49) Mojzisova, H.; Bonneau, S.; Vever-Bizet, C.; Brault, D. *Biochim. Biophys. Acta* **2007**, *1768*, 366–374.
(50) Seelig, A.; Gerebtzoff, G. *Expert Opin. Drug Metab. Toxicol.* **2006**, *2*(5), 733–752.
(51) Heerklotz, H.; Binder, H.; Lantzsch, G. *J. Fluoresc.* **1994**, *4*(4), 349–352.
(52) Wiehe, A.; Simonenko, E. J.; Senge, M. O.; Röder, B. *J. Porphyrins Phthalocyanines* **2001**, *5*, 758–761.

signal ($k = 0.5 \times 10^{-5}$ s^{-1}, Figure 6B). Other factors in addition to transbilayer distribution may contribute to the observed signal narrowing of the *outer* $-N^+(CH_3)_3$ group, for example, solely a deeper penetration of the chlorin molecule within the outer lipid layer toward the hydrophobic core without subsequent translocation. This may also cause the temporal decrease of $\nu_{1/2,outer}$ in the presence of MACE (Figure 6C), which apparently does not cross the membrane. A similar behavior has been postulated for a *cis*-disulfonated phthalocyanine (PcS_2Al), which did not tend to cross the membrane but slowly seemed to penetrate deeper into the lipidic core of the vesicle.[9] The temporal progression of $\nu_{1/2,inner}$ passes through a maximum before leveling off to its limiting value in the presence of CE (Figure 6B). Even though hypothetical, a possible reason for this curve progression may be as follows: First, increasing CE concentration in the inner membrane layer ($[CE]_{inner}$) increases chemical shift anisotropy (CSA) relaxation of DOPC choline protons, leading to signal line broadening. Second and superimposed, dynamic effects may be responsible for the subsequent line width decrease: An exchange at intermediate rate (on the NMR time scale) between PL molecules either unoccupied or occupied with CE in the inner leaflet may result in maximum line broadening at $[CE]_{inner}$ where the two possible populations (with CE occupied/unoccupied PL) are more or less equal. A corresponding simulation of such a dynamic process with $\nu_{1/2,inner} = f([CE]_{inner})$ using experimental values, that is, initial and final $\delta(-N^+(CH_3)_{3,inner})$ and $\nu_{1/2,inner}$ as start parameters and assuming an intermediate exchange rate constant, resulted in a similar curve progression as the experimental curve, supporting the above hypothesis.

4.2. Steps Involved in Kinetics of Chlorin Membrane Interaction. Various steps may be involved in the kinetic process comprising chlorin vesicle interactions. The first step is characterized by the adsorption and subsequent entry of a fraction of the available chlorin from the aqueous bulk phase into the outer vesicle monolayer. This adsorption to the outer membrane layer is governed by the high binding affinity of the amphiphilic chlorin molecules CE and MACE toward the model membrane as was indicated by the distribution coefficients determined for CE and MACE (Figure 4). This first step, chlorin adsorption to the outer vesicle monolayer, takes place very quickly, too fast to be followed by NMR, and is reported to be diffusion controlled with the adsorption rate being independent of the pH and ionization state of the porphyrin.[53] In our kinetic experiments, it presents the initial state at time zero. It is mainly characterized by the split $-N^+(CH_3)_3$ resonance appearing immediately after chlorin addition.

The second much slower step comprises chlorin distribution between the outer and inner vesicle monolayers. This transbilayer distribution is governed by the concentration gradient of chlorin in the outer and inner PL monolayer at time *t*. The rate of CE movement to the inner monolayer to reach equilibrium seems to follow first-order kinetics. The concentration of free, that is, with CE unoccupied DOPC from the inner membrane layer, as reflected by the chemical shift of the corresponding protons, decreases exponentially to its value at equilibrium, which is determined by the uptake capacity for CE. The reverse transfer, that is, the equilibration with movement of CE from the inner membrane layer back toward the outer, is, at least initially, most likely strongly repelled, since the concentration of CE in the inner enclosed aqueous volume is close to zero. Sites becoming vacant in the outer monolayer upon movement of chlorin toward the inner layer are presumably replaced by fast binding of excess chlorin from the aqueous bulk phase. Taking the size and the amphiphilic structure of the chlorin molecule into account, distribution between the membrane layers takes place by a flip-flop mechanism rather than by diffusion along the membrane interior toward the inner hemileaflet.[13,54] In analogy, membrane transfer by a flip-flop mechanism has been suggested for deuteroporphyrin across dimyristoylphosphatidylcholine (DMPC)[11] and partially unsaturated bilayers[13] and for other amphiphilic compounds.[54−57]

In a third step, a small fraction of chlorin now residing in the inner vesicle monolayer may exit into the enclosed aqueous volume to reach equilibrium between CE in the vesicular and aqueous phase. However, due to the high distribution coefficient of CE, this equilibrium most likely is strongly shifted toward the vesicle phase.

4.3. Comparison of CE with MACE and Other Solutes with Respect to Their Membrane Transfer Kinetics. The average half-life for the CE transbilayer flip-flop process was found to be in the range of several hours (23 h at CE/DOPC = 0.3 and 108 h at CE/DOPC = 0.025) at neutral pH (pH 7.10 ± 0.05). The slow transfer rate found for CE is in agreement with preliminary results obtained by Mojzisova et al.[49] from fluorescence studies suggesting a very slow distribution of chlorin e6 as opposed to deuteroporphyrin, a dicarboxylic porphyrin, with a much higher rate constant ($\sim 10^{-2}$ s^{-1}).[13] Fitting of either the chemical shift or line width data of the inner choline signal versus time to a monoexponential function yields flip-flop rate constants for CE in the order of $10^{-5}-10^{-6}$ s^{-1}, that is, about 3−4 orders of magnitude slower than that of deuteroporphyrin. The slow flip-flop rates found for CE in our study are comparable to those reported for cholesterol and certain phospholipids with half-lives in the range of minutes to hours.[58,59] Among the PLs, especially phosphatidylcholine (PC) and phosphatidylinositol (PI) derivatives have been reported to translocate across the membrane with half-lives of several hours.[60,61] Thus, the flip-flop of DOPC molecules may take place simultaneously to the flip-flop of CE. However, DOPC flip-flop is not observable in the experimental setup of the present study as long as the DOPC movements do not take place unevenly. This would result in a shift of the integral ratios of outer and inner choline signals which were found to remain equal over time though. Moreover, uniform DOPC exchange between the inner and outer membrane layer is unlikely to affect only CE but not MACE transbilayer movement, considering the differences found for both chlorin compounds.

In contrast to the case of CE, MACE seemed to remain attached to the membrane surface without crossing the lipid bilayer at neutral pH and a molar ratio MACE/DOPC of 0.3 (Figures 5 and 6). The observed difference between CE and MACE must be due to the above-discussed differences in the chemical structure: The distribution from the aqueous into the vesicular phase was found to be higher for CE than for MACE most likely due to the increased hydrophobicity of CE. Accordingly, it can be obtained from literature values that log *P* values (octanol/water partition coefficients) of CE and MACE differ substantially by

(53) Vever-Bizet, C.; Brault, D. *Biochim. Biophys. Acta* **1993**, *1153*, 170–174.
(54) Regev, R.; Eytan, G. D. *Biochem. Pharmacol.* **1997**, *54*, 1151–1158.
(55) Homan, R.; Pownall, H. J. *Biochim. Biophys. Acta* **1988**, *938*, 155–166.
(56) Kessel, A.; Musafia, B.; Ben-Tal, N. *Biophys. J.* **2001**, *80*, 2536–2545.
(57) Hamilton, J. A. *J. Lipid Res.* **1998**, *39*, 467–481.
(58) Smith, R. J. M.; Green, C. *FEBS Lett.* **1974**, *42*, 108–111.
(59) Middleton Boon, J.; Smith, B. D. *J. Am. Chem. Soc.* **1999**, *121*, 11924–11925.
(60) Bütikofer, P.; Lin, Z. W.; Chiu, D. T.-Y.; Lubin, B.; Kuypers, F. A. *J. Biol. Chem.* **1990**, *265*, 16035–16038.
(61) Middelkoop, E.; Lubin, B. H.; Op den Kamp, J. A.; Roelofsen, B. *Biochim. Biophys. Acta* **1986**, *855*, 421–424.

a factor of 75 (CE/MACE, pH 7.2).[62] However, owing to its amphiphilic structure, MACE still has an affinity high enough to associate with the outer DOPC monolayer. Strong electrostatic interactions between the carboxylate side chains and the positively charged DOPC choline groups seem to be responsible for the retention of MACE in the outer leaflet. Different polarities and hence different binding affinities to the polar part of DOPC also affect flip-flop rate constants. The increase in flip-flop rate from MACE bearing four carboxy groups to CE bearing three carboxy groups corresponds to the increase in flip-flop rate from CE to that reported for deuteroporphyrin[13] bearing only two carboxy groups. These data suggest that in general the addition of just one more carboxylic group to the polar side of the amphiphilic molecule may decrease the membrane transition rate constant of the corresponding porphyrin by several orders of magnitude. In analogy to the case of MACE, pure adsorption to the membrane surface without crossing the bilayer has been reported for disulfonated aluminum phthalocyanine (PcS_2Al) which was attributed to the two negatively charged sulfonate groups at the ring periphery.[9] Similarly, a comparative study on the flip-flop of phospholipids of various polarities has come to the conclusion that the *polar moiety* of the translocating compound accounts for the major barrier to transmembrane movement.[63]

5. Concentration Dependence of CE Distribution across the DOPC Bilayer. *5.1. Quantitative Distribution of CE across the Bilayer as a Function of CE Concentration.* In the present study, a clear positive correlation between the extent of asymmetry and CE concentration was found (Figure 8B). Complete merging of the split methyl choline peaks indicating equal CE distribution between the inner and outer monolayer was only observed at a low CE concentration (Figure 8B), that is, a molar ratio CE/DOPC of 0.025 (see also Figure 5). As the CE concentration is increased, an increasing shift difference of the inner and outer choline signal remains at equilibrium. Potential reasons for this remaining split at high CE/DOPC ratios may be as follows: (i) The higher packing density of DOPC molecules in the inner vesicle layer may lead to different chlorin attachment between inner and outer membrane layers and hence to a different chemical shift. (ii) CE may be asymmetrically distributed between the inner and outer membrane leaflet at high CE concentrations with more CE residing in the outer hemisphere. The above-mentioned differences in DOPC packing density between inner and outer membrane layers could also be responsible for such an asymmetric CE distribution.

Asymmetric distribution between the inner and outer leaflets has also been reported for certain lipid components within biomembranes[60,64,65] but also within synthetic PL vesicles, for example, for α-tocopherol,[66] cholesterol,[67] and phosphatidylethanolamine (PE).[68] While in cell membranes other membrane components or active transport mechanisms may contribute to maintain such an asymmetry,[65] in vesicles membrane curvature[69,70] or concentration effects[66,67] have been suggested as possible reasons for transbilayer asymmetry.

Finally, the limited uptake of chlorin (Figure 4), the continuous correlation between chlorin concentration and the initial split (Figure 8A), as well as the remaining split of the DOPC choline signal at high CE concentrations (Figure 8B) all indicate that the vesicle integrity seems to be maintained under the experimental conditions. Moreover, the DOPC distribution in the inner and outer vesicle layers in the presence of chlorin was found to remain almost equal as compared to chlorin-free vesicles, and only small changes in vesicle size were observed upon CE addition even at the highest molar ratio CE/DOPC.

5.2. Rate of CE Transfer as a Function of CE Concentration. Reciprocal half-lives $t_{1/2}^{-1}$, which are proportional to the flip-flop rates, were found to depend on the molar ratio of CE/DOPC or on the CE concentration in the outer monolayer (Figure 9A). $t_{1/2}^{-1}$ values increased from about 0.3×10^{-5} s^{-1} at CE/DOPC $= 0.025$ to about 1.6×10^{-5} s^{-1} at CE/DOPC $= 0.6$ (Figure 9A). This flip-flop acceleration may be promoted simply by the high CE concentration or by increasing packing constraints in the outer hemileaflet at higher CE concentrations. Accordingly, other reports have suggested that such mechanical stress induced by the uptake of large amounts of a compound into the outer membrane layer contributes to an increase in flip-flop rates, thereby relieving the differential packing density.[71,72]

While in both cases, at low and high CE/DOPC ratio, the *inner* $-N^+(CH_3)_3$ resonance position exhibited a similar time course, the *outer* $-N^+(CH_3)_3$ resonance positions proceeded differently (Figure 6A, B). At CE/DOPC $= 0.025$, the *outer* $-N^+(CH_3)_3$ resonance continuously shifts downfield, indicating depletion of CE in the outer monolayer due to CE migration toward the inner layer until equilibrium is reached (Figure 6A). At CE/DOPC $= 0.3$, the temporal displacement of the outer $-N^+(CH_3)_3$ resonance is less pronounced and initially even moves further upfield before shifting toward the inner choline signal (Figure 6B). This indicates that CE translocation to the inner membrane layer seems to be more efficiently replaced by excessive CE in the aqueous bulk phase.

6. Rate of CE Transfer as a Function of Cholesterol Mole Fraction. The addition of cholesterol to PL membranes results in a concentration-dependent increase in membrane rigidity, with the mobility of the PL alkyl chain being more restricted than that of the PL headgroup.[19] Lindblom et al. observed a decrease in the lipid lateral diffusion coefficient and an increase of ordering of DOPC bilayers if cholesterol is added.[73] This increase in membrane rigidity led in our study to a significant decrease of the average reciprocal half-lives with increasing cholesterol addition (Figure 9B). The amount of CE bound to the vesicle outer layer was found to be slightly enhanced with increasing cholesterol content. In contrast, for *cholesterol-free* DOPC vesicles, the flip-flop rate was found to increase with CE concentration. Therefore, it is very unlikely that the observed decreased transbilayer movement of CE is due to a concentration effect of CE bound to the vesicles. This result demonstrates that, in addition to structural parameters of the porphyrin, membrane fluidity has a profound effect on the flip-flop rate constant. Moreover, the correlation between cholesterol content and temporal distribution of CE provides further evidence for the assumed kinetic model with respect to chlorin flip-flop. In agreement with our results, a strong decelerating effect on the transbilayer flip-flop rate constants of deuteroporphyrin[12] and other compounds[9,24,54] due to the presence of cholesterol has been described.

(62) Kessel, D. *Photochem. Photobiol.* **1989**, *49*, 447–452.
(63) Homan, R.; Pownall, H. J. *Biochim. Biophys. Acta* **1988**, *938*, 155–166.
(64) Kiessling, V.; Crane, J. M.; Tamm, L. K. *Biophys. J.* **2006**, *91*, 3313–3326.
(65) Zachowski, A. *Biochem. J.* **1993**, *294*, 1–14.
(66) Bellemare, F.; Fragata, M. *J. Membr. Biol.* **1981**, *58*, 67–74.
(67) De Kruijff, B.; Cullis, P. R.; Radda, G. K. *Biochim. Biophys. Acta* **1976**, *436*, 729–740.
(68) Sarti, P.; Molinari, A.; Arancia, G.; Meloni, A.; Citro, G *Biochem. J.* **1995**, *312*, 643–648.
(69) Rovira-Bru, M.; Thompson, D. H.; Szleifer, I. *Biophys. J.* **2002**, *83*, 2419–2439.
(70) Nordlund, J. R.; Schmidt, C. F.; Dicken, S. N.; Thompson, T. E. *Biochemistry* **1981**, *20*, 3237–3241.
(71) Donovan, J. M.; Jackson, A. A. *Biochemistry* **1997**, *36*, 11444–11451.
(72) Raphael, R. M.; Waugh, R. E. *Biophys. J.* **1996**, *71*, 1374–1388.
(73) Lindblom, G.; Orädd, G.; Filippov, A. *Chem. Phys. Lipids* **2006**, *141*, 179–184.

7. Significance and Limitations of the Presented Model Studies. Phospholipid bilayer vesicles are being widely used as simple cell membrane models to study drug−membrane interactions.[74,75] In the present study, intermediate sized unilamellar vesicles were chosen, because these model systems retain the essential lipid bilayer structure of biological cell membranes while at the same time the dynamic properties, that is, fast tumbling in solution, allow one to obtain relatively well-resolved NMR signals. The extrusion method provides vesicles exhibiting highly reproducible properties with respect to size and size distribution, and they can be easily and rapidly obtained. However, some restrictions of using vesicles as membrane models apply: These are mainly due to the membrane curvature and resulting packing constraints as well as to the membrane constituents. Considering on one hand the vesicle size (50−60 nm) and a membrane thickness of 3.7 nm[76] and on the other hand that the PL molecules are almost evenly distributed, the PL molecules are obviously more densely packed in the inner sphere. However, the curvature of the vesicles is obviously not sufficient to cause strong packing constraints, because these cause splitting or shoulders of the PL ^{1}H NMR signals[77] which was not observed for the DOPC spectra in this study (see Figure 2A). Nevertheless, a certain limitation of the current study is that values obtained for membrane distribution kinetics may and are assumed to vary depending on the nature of the applied membrane model.[64,78,79] For example, flip-flop rates of fatty acids have been reported to correlate with vesicle size[57,78,80] which was attributed to membrane curvature; that is, translocation was slowed down in planar bilayers as compared to spherical vesicles. Moreover, membranes are complex mixtures, and even though porphyrin accumulation in PDT is known to be unspecific encompassing different kinds of membranous structures, other components but phospholipids may contribute to porphyrin membrane interactions. The vesicle model applied in the present study simplifies the membrane complexity, allowing one to focus on the role of just one individual component, namely, the phospholipid bilayer, in chlorin membrane interactions.

Part of the data reported in the present study was obtained at molar chlorin to phospholipid ratios between 0.025 and 0.3 corresponding to absolute chlorin concentrations in the final vesicle solutions of 0.15−2.4 mg/mL. In particular, the upper limit of this concentration range is clearly higher than that of actual in vivo drug to membrane ratios. For example, MACE is administered at concentrations of 25 mg/mL saline at doses up to 3.5 mg/kg to human subjects with resulting serum levels of around 0.02 mg/mL about 1 h after bolus infusion.[81] The high state of occupancy of DOPC vesicles with chlorin molecules at a molar ratio of 0.3 in the present study may alter the properties of the PL bilayer and thus may influence the flip-flop kinetics, therefore possibly limiting the comparability with physiological conditions at least after distribution of chlorin in the body. Even though the continuous changes observed for chlorin-concentration-dependent data (see, e.g., Figure 8) suggest preservation of the membrane structure, it cannot be excluded that the PL bilayer may likewise undergo continuous changes. However, for both low (0.025) and high (0.3) molar ratios, a similar kinetic profile could be observed for CE transbilayer movement (Figure 6). This comparability of low and high molar ratios is also supported by yet unpublished data obtained at different pH values. Moreover, the order of magnitude found for CE flip-flop across membranes is in agreement with preliminary results obtained by fluorescence spectroscopy applying much lower porphyrin concentrations.[49] Nevertheless, keeping the above restrictions in mind, the model proves to be well-suited to reveal the significant differences between CE and MACE transbilayer movement found under the same experimental conditions regardless of the exact absolute values of rate constants. Moreover, both the qualitative kinetic profile and the order of magnitude of flip-flop rates were found to be valid for both low and high chlorin to membrane ratios, and it may thus be justified to project the results to in vivo conditions.

Conclusions

In the present study, ^{1}H NMR spectroscopy was used to determine kinetic rates for porphyrin flip-flop processes across model membranes. In addition, the NMR data provided information on the aggregation behavior, distribution coefficients, membrane affinity, and preferred localization in the model membrane of the investigated chlorin compounds. The knowledge of these factors is important for correlating porphyrin structure with PDT efficacy as well as with cellular uptake and subcellular distribution pathways. MACE was found to be retained in the outer membrane layer, while CE distributed relatively slowly across the lipid bilayer. The flip-flop rate found for CE at neutral pH most likely is too slow for cellular uptake of CE by passive diffusion. Thus, both chlorins presumably are taken up by the cell via the endocytotic pathway. Accordingly, MACE has been reported to localize in lysosomes, indicating endocytotic uptake.[1,62] However, owing to the differences in polarity and different lipoprotein binding properties reported in the literature,[49,62,82] CE is more likely to adopt the LDL-receptor-mediated pathway, while MACE may rather be internalized by the cell via pinocytosis.[2] Thus, combining the presented data with previous findings,[62,82] neither passive diffusion nor high incidence of LDL receptors may be responsible for enhanced uptake of MACE by proliferative tissue. Other mechanisms, for example, the abnormal structure of tumor stroma,[2] may be more relevant for tumor selectivity of MACE.

Comparing the time-dependent membrane distribution found for MACE and CE with that reported for deuteroporphyrin[13] allows predictions to be made about the structural requirements of amphiphilic porphyrins for fast diffusion across the membrane. In this regard, the number of ionizable groups was found to have a pronounced effect on the membrane transfer rate.

CE was found to bind more efficiently to the outer membrane layer than MACE. At the same time, CE interactions with the polar headgroup region of DOPC are weaker than those for MACE, enabling CE to distribute across the hydrophobic core of the membrane to equilibrate between the inner and outer membrane layers. Porphyrin- and light-induced formation of short-lived singlet oxygen, which is the active species causing membrane damage, ideally takes place at the desired site of action, that is, in the membrane interior.[4] Therefore, properties such as high membrane affinity and membrane penetration are favorable for PDT drugs targeting subcellular membranes. In fact, the plasma membrane has been reported to be a cellular accumulation site of free chlorin e6.[83] However, despite the lack

(74) Seydel, J. K.; Wiese, M. *Drug-Membrane Interactions*; Wiley-VCH Verlag GmbH: Weinheim, 2002.
(75) Zepik, H. H.; Walde, P.; Kostoryz, E. L.; Code, J.; Yourtee, D. M. *Crit. Rev. Toxicol.* **2008**, *38*, 1–11.
(76) Kučerka, N.; Uhríková, D.; Teixeira, N.; Balgavý, P. *Physica B* **2004**, *350*, e639−e642.
(77) Brouillette, C. G.; Segrest, J. P.; Ng, T. C.; Jones, J. L. *Biochemistry* **1982**, *21*, 4569–4575.
(78) Kleinfeld, A. M.; Storch, J. *Biochemistry* **1993**, *32*, 2053–2061.
(79) Pohl, E. E.; Peterson, U.; Sun, J.; Pohl, P. *Biochemistry* **2000**, *39*, 1834–1839.
(80) Kleinfeld, A. M.; Chu, P.; Romero, C. *Biochemistry* **1997**, *36*, 14146–14158.
(81) Chan, A. L.; Juarez, M.; Allen, R.; Volz, W.; Albertson, T. *Photodermatol., Photoimmunol. Photomed.* **2005**, *21*, 72–78.

of deep membrane penetration, MACE has been reported to act as an efficient photosensitizer.[2] Therefore, different targets or mechanisms of action may underlie photodynamic tissue damage caused by CE and MACE. In conclusion, the knowledge of the structure-dependent membrane interactions and kinetics, as exemplified in the present study for CE and MACE, may aid in exploring the principles underlying PDT and substantially contribute to improved target-oriented design of new photosensitizers.

(82) Èunderliková, B.; Kongshaug, M.; Gangeskar, L.; Moan, J. *Int. J. Biochem. Cell Biol.* **2000**, *32*, 759–768.

(83) Akhlynina, T. V.; Rosenkranz, A. A.; Jans, D. A.; Sobolev, A. S. *Cancer Res.* **1995**, *55*, 1014–1019.

Acknowledgment. Support was obtained from the Swiss National Science Foundation (SNF), Grant Nos. MHV 2134-068576 and 2000-061377. U.S. acknowledges funding from NIH and NSF (NIH MBRS SCORE S06 GM052588-12 & S06 GM052588-09S1, NSF DBI 0521342).

Supporting Information Available: Determination of inside−outside distribution of DOPC phospholipids in DOPC vesicles using the lanthanide shift reagent $PrCl_3$ by ^1H NMR spectroscopy; determination of vesicle size before and after chlorin addition at various molar ratios chlorin/DOPC and as a function of time by dynamic light scattering (DLS). This material is available free of charge via the Internet at http://pubs.acs.org.

LA802040V